

## Incorporating human factors into LCM using fuzzy TCI model

Linbo Li , Yang Li & Daiheng Ni

To cite this article: Linbo Li , Yang Li & Daiheng Ni (2021) Incorporating human factors into LCM using fuzzy TCI model, Transportmetrica B: Transport Dynamics, 9:1, 198-218, DOI: [10.1080/21680566.2020.1837033](https://doi.org/10.1080/21680566.2020.1837033)

To link to this article: <https://doi.org/10.1080/21680566.2020.1837033>



Published online: 24 Oct 2020.



Submit your article to this journal [↗](#)



Article views: 45



View related articles [↗](#)



View Crossmark data [↗](#)



# Incorporating human factors into LCM using fuzzy TCI model

Linbo Li<sup>a</sup>, Yang Li<sup>a</sup> and Daiheng Ni<sup>b</sup>

<sup>a</sup>Key Laboratory of Road and Traffic Engineering of Ministry Education, Tongji University, Shanghai, People's Republic of China; <sup>b</sup>Civil and Environmental Engineering, University of Massachusetts Amherst, Amherst, MA, USA

## ABSTRACT

Incorporation of Human Factors (HF) into the mathematical car-following (CF) models has always been the research hotspot. Ignorance of such inclusion would inevitably hinder us from acquiring a comprehensive understanding of traffic flow phenomena. This paper proposed a novel CF model in order to bridge three existing research gaps: the demand for more inclusion of HF into the Longitudinal Control Model (LCM); the requirement for a more desirable underlying CF model for the Task Capability Interface (TCI) model; the ignorance of the fuzziness of human brains when modeling Task Difficulty (TD). Specifically, in order to imitate driver's natural or subjective uncertainty and ambiguity of his TD, the fuzzy logic approach is introduced, and the TD is then incorporated into the LCM. Thereafter, both numerical simulation and field-data validation have been performed. Results indicate that our proposed model is more capable of accommodating HF and exhibits better performance than its predecessor.

## ARTICLE HISTORY

Received 12 May 2020  
Accepted 11 October 2020



## KEYWORDS

Car-following model; human factors; task capability interface model; fuzzy logic algorithm

## 1. Introduction

As one of the core components of microscopic traffic flow theory, car-following (CF) theory describes the longitudinal interaction between the following vehicle and the front vehicle (Ni 2016a). CF events can be observed constantly in real traffic environment, and they could exert significant impacts on traffic flow dynamics and safety (Brackstone and McDonald 1999; Saifuzzaman and Zheng 2014; Ni 2016a). Researching on CF behavior can not only help us understand the essence and characteristics of traffic phenomena, but also enable us develop more reliable automatic CF algorithms with the advent of autonomous vehicles (Wu, Wang, and Li 2020; Calvert and Van Arem 2020). Therefore, it is essential for us to have a comprehensive understanding and accurate modeling of CF behavior.

After the pioneering CF model proposed by Pipes (1953) and Reuschel (1950), numerous methods (Gazis, Herman, and Rothery 1961; Wiedemann 1974; Gipps 1981; Fritzsche 1994; Treiber, Kesting, and Helbing 2006; Ossen and Hoogendoorn 2006; Andersen and Sauer 2007; Yang and Peng 2010; Przybyla, Taylor, and Jupe 2012; Chen et al. 2016; Van Lint, Calvert, and Schakel 2017; Batool, Mubasher, and ul Qounian 2019) have been proposed to model CF behavior over the past decades, such as the well-known stimulus–response model (Gazis, Herman, and Rothery 1961), which models driver's response as the product of his sensitivity and stimulus; the optimal velocity model family (Bando et al. 1995; Jiang, Wu, and Zhu 2001), which assumes driver would adjust their current speed to their desired speed; the famous safety-distance-based model (Gipps 1981), which assumes driver would maintain a large enough safe headway to avoid collision in case the leader car brakes unexpectedly; the psycho-physical models (Wiedemann 1974; Fritzsche 1994), which attempt to introduce the term 'perceptual

**CONTACT** Yang Li  cc960719@tongji.edu.cn  Key Laboratory of Road and Traffic Engineering of Ministry Education, Tongji University, 4800 Cao'an Road, Shanghai 201804, People's Republic of China

threshold' to imitate driver's weakness of perceiving trivial changes in their driving environment; the DVA (Driving by Visual Angle) model (Andersen and Sauer 2007), which attempts to model driver's stimulus as the change of the visual angle of the leader car; modeling driver's perception errors in estimating his driving environment (Treiber, Kesting, and Helbing 2006; Van Lint, Calvert, and Schakel 2017); and modeling traffic collisions through incorporating distraction into the CF models (Yang and Peng 2010; Przybyla, Taylor, and Jupe 2012) etc. For a detailed review of existing CF models, please refer to Brackstone and McDonald (1999) and Saifuzzaman and Zheng (2014).

Admittedly, existing researches in modeling CF behavior have achieved notable results. However, researchers are still facing the challenge of incorporating more human factors into the CF models as criticized in Saifuzzaman and Zheng (2014). If existing researches fail to surmount this shortcoming, then it is difficult for the existing CF models to fully reproduce the characteristics of actual traffic flow environment, thus hindering us from understanding the essence and characteristics of traffic phenomena comprehensively. Among one of the efforts intended to bridge this research gap, one approach is to incorporate Risk Allostasis Theory (RAT) (Fuller 2005, 2011) into current CF models (Hoogendoorn et al. 2013; Saifuzzaman, Zheng, and Haque 2015, 2017; Van Lint and Calvert 2018; Batool, Mubasher, and ul Qounian 2019) using the well-known framework of the Task Capability Interface (TCI) model (Fuller 2005, 2011).

RAT stipulates that the most important motivation influencing drivers' decisions may be classified under task demand elements, and it also argues that driver's control actions at each moment are primarily influenced by the desire to maintain perceived risk within his acceptable range (Fuller 2005, 2011). Driver's sense of risk could be modeled as task difficulty using the TCI model (Fuller 2005), which assumes driver must ensure that the total task demands at each moment should within his or her capability (Fuller 2011) as illustrated in Figure 1. Driver's task difficulty is the result of dynamic interactions between driver's task capability and task demand. In addition, driver's task demand can be divided into: driving task demand (car-following or lane-changing task) and non-driving task demand, which can also be called secondary task (Precht, Keinath, and Krems 2017). Therefore, driver's task difficulty can be roughly divided into three cases: (1) If driver's total task demands are within his task capability, the driver can easily deal with his current tasks demands; (2) If driver's total task demands approach his task capability, the driver may feel that it is difficult to complete his current tasks; (3) If driver's total task demands exceed his task capability, the driver may feel unable to handle his current tasks, which may lead to traffic collisions.

Hoogendoorn et al. (2013) made the first attempt to incorporate the TCI model into the IDM (Intelligent Driver Model). The novel theoretical framework is developed and implemented to the IDM. Simulation results demonstrate the effect of a changing balance between driver's driving task demand and driver's capability. Thereafter, Saifuzzaman, Zheng, and Haque (2015) presented a detailed formulation of driving task difficulty, which is modeled as the ratio between driver's desired time headway and the actual headway, assuming driver would increase his desired headway with the increase of the driving task difficulty. Hereafter, this item is introduced to modify the Gipps and IDM CF models, which are then named as TDGipps and TDIDM respectively. Using the same method, this correction method was also applied to the FVD model in Batool, Mubasher, and ul Qounian (2019). Recently, Van Lint and Calvert (2018) extended the research in TCI model and proposed a multi-level modelling and simulation framework. Their research redefines the task demand as the amount of information processing costs needed to fulfill a task, and defines task capacity as the driver's capacity for information processing capacity (Van Lint and Calvert 2018; Calvert and Van Arem 2020). Furthermore, they assume the increase of driver's task demand would cause the deterioration of driver's SA (situational awareness) (Endsley 1995). This kind of deterioration in awareness would result in the increase of driver's perception errors and reaction time. Meanwhile, driver's response adaption would change in terms of desired speed, headway, etc. Thereafter, the degree of such deterioration is used to modify the parameters in IDM, thus driving task demand and non-driving task demand could be endogenously modeled in the existing CF models.

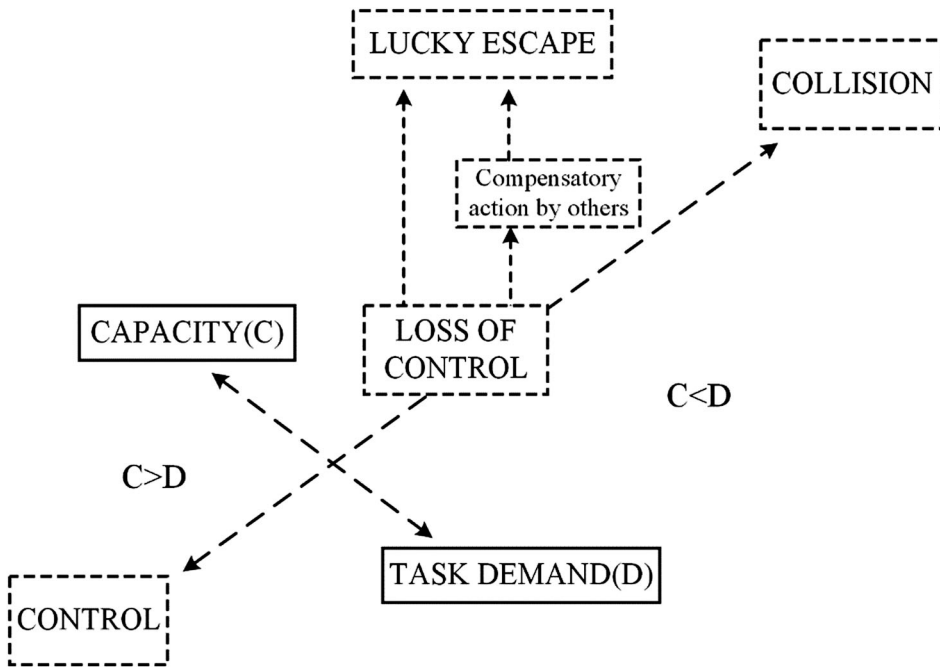


**Figure 1.** The framework of the Task Capability Interface Model (Fuller 2005).

Inspired by the existing researches of incorporating the framework of the TCI model into the existing CF models (Hoogendoorn et al. 2013; Saifuzzaman, Zheng, and Haque 2015, 2017; Van Lint and Calvert 2018; Batool, Mubasher, and ul Qounian 2019), a novel CF model has been proposed in this paper. Although the above literatures have achieved certain results, the approaches of using the deterministic mathematical equations to replicate driver's task difficulty may fail to consider the uncertainties and ambiguities in driver's perception and decisions (Khodayari et al. 2011; Hao, Ma, and Xu 2016). This inevitably makes the above models difficult to truly reflect this human factor. While the fuzzy logic approach is capable of modeling such human behavior, and this approach is consistent with the fuzziness of human brains. It could better reflect driver's natural or subjective perceptions of inputs from his driving environment. Therefore, we introduce the fuzzy logic approach to formulate driver's task difficulty in this paper, and we mainly focus on modeling the driving (car-following) task difficulty.

On the other hand, their selection of the underlying CF model for the TCI model deserves further discussion. The desirable underlying CF model should be simple, efficient, generalized and, more importantly, should be based on a sound theoretical background. Unfortunately, this is not well manifested in the existing literatures. In order to improve this limitation, we introduce the LCM (Longitudinal Control Model) as the underlying model for the incorporation of the above obtained task difficulty. The LCM model has many good properties (physically meaningful, simple, flexible, consistent and valid) (Ni, Leonard, and Jia 2015), and more importantly, it has perfect theoretical support (it is derived from a combined perspective of physics and human factors, as shown in Figure 2) (Ni, Leonard, and Jia 2015). At the same time, a unified perspective (Ni 2016b) has been casted on the existing microscopic traffic flow models (existing CF models can be related to each other conveniently). Therefore, it is desirable for us to adopt this model as the underlying model for the framework of the TCI model. However, although the LCM model has many good properties, this model still has rooms worthy of improvements in incorporating more human factors, and few studies have tried to do this so far. Therefore, it is also advisable for us to incorporate task difficulty into the LCM model in order to make more inclusion of human factors.

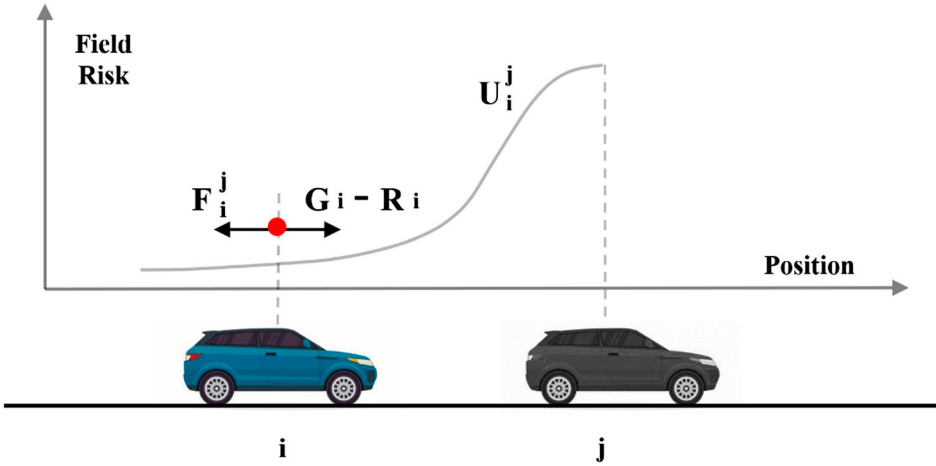


**Figure 2.** The field perceived by driver  $i$  in the longitudinal direction.

Consequently, the formulation of our proposed model mainly consists of: (1) introduction of fuzzy logic approach to imitate driver's task difficulty; (2) introduction of LCM as the underlying model for the incorporation of task difficulty. The establishment of our model is in the context of our attempts to bridge the above three research gaps (the demand for more inclusion of human factors into the LCM model; the requirement for a more desirable underlying CF model for the framework of the TCI model; the ignorance of the fuzziness of human brains when modeling driver's task difficulty). Through the combination of these approaches, the framework of the TCI model and the LCM model could be viewed as complementary to each other, and the formulation of task difficulty could truly reflect the fuzziness of driver brains, thus making our proposed model has greater potential in reflecting the actual traffic characteristics.

Finally, we have designed a feasible genetic algorithm to calibrate the parameters of the proposed model. Meanwhile, a comparison between the proposed model and its predecessor has been also made so as to evaluate the performance of our proposed model. Results suggest that our proposed model exhibits better performance than its predecessor in reproducing the actual traffic characteristics. The remainder of this paper is organized as follows. Section 2 presents the formulation of the proposed FTD-LCM model. The numerical experiments are shown in Section 3. Section 4 presents the calibration preparation of the proposed model. The calibration and validation results are presented in Section 5. The discussion of this paper is presented in Section 6. Finally, the conclusion is given in Section 7.

## 2. The formulation of the proposed model

### 2.1. Longitudinal control model

Field Theory (Ni 2016b) represents everything in the environment (highways and vehicles) as a field perceived by the subject driver whose mission is to achieve his or her goals by navigating through the overall field. The LCM (Longitudinal Control Model) is derived through focusing the forces for the vehicle in the longitudinal direction. For further details of the generic form of the Field Theory, please refer to Ni (2016b). The mathematics formula of the LCM is given below:

$$\ddot{x}_i(t + \tau_i) = A_i \left[ 1 - \frac{\dot{x}_i(t)}{v_i} - e^{1-s_{ij}(t)/s_{ij}^*(t)} \right] \quad (1)$$

$$s_{ij}^*(t) = \frac{\dot{x}_i^2(t)}{2b_i} - \frac{\dot{x}_j^2(t)}{2B_j} + \dot{x}_i(t)\tau_i + L_j \quad (2)$$

Where  $i$  denotes the follower vehicle,  $j$  denotes the leader vehicle,  $\ddot{x}_i(t)$  denotes current acceleration,  $\dot{x}_i(t)$  denotes current velocity,  $L_i$  denotes the vehicle length,  $\tau_i$  denotes the reaction time,  $s_{ij}(t) = x_j(t) - x_i(t)$  denotes the spacing between vehicle  $i$  and  $j$ ,  $\Delta\dot{x}_{ij}(t) = \dot{x}_j(t) - \dot{x}_i(t)$  denotes the relative velocities,  $v_i$  denotes the desired speed,  $A_i$  denotes the maximum acceleration,  $s_{ij}^*$  denotes the desired safe spacing of driver  $i$ ,  $\dot{x}_i^2(t)/2b_i - \dot{x}_j^2(t)/2B_j$  denotes the driver's aggressiveness,  $b_i$  denotes the maximum deceleration that the driver can confidently apply in an emergency,  $B_j$  denotes the driver's estimation of the leader vehicle's comfortable deceleration in an emergency brake.

## 2.2. Basic constructs of the proposed model

Under the framework of the TCI model, task difficulty arises out of the dynamic interaction between driver's task demands and driver's task capability (Fuller 2005). Driver's capability is initially constrained by biological characteristics of the driver, such as information processing capacity and speed, reaction time, physical reach, motor coordination and perhaps flexibility and strength (Fuller 2005). In general, driver's task demands can be divided into: Driving task demand (i.e. car-following task or lane-changing task) and Non-driving task demand (not related to driving, like answering the phone or chatting with passengers, etc.). In line with the TCI model, Van Lint and Calvert (2018) define task demand and task capacity as the amount of information processing effort needed to fulfill a task and driver's information processing capacity. Meanwhile, task saturation is introduced to gauge the degree in which this workload 'saturates' drivers' capability. Furthermore, based on the dynamic SA (situational awareness) model in Endsley (1995), three levels of SA are then modeled in the generic framework. The saturation of the (driving task and non-driving task) workload for the driver may lead to the deterioration of his SA (Fuller 2005; Van Lint and Calvert 2018; Wickens, Hollands, and Banbury 2015). The deterioration of driver's SA may result in the perception errors of the surroundings (i.e. spacing distance and relative velocity with the leader vehicle), and it may trigger driver's behavior responses (i.e. reaction time, desired speed).

$TD_{\text{car-following}}$  is defined as the information processing cost when the driver attempts to maintain his driving task in the longitudinal direction (the lateral driving task mainly refers to the lane-changing driving task, which is beyond the research scope of this paper).  $TD_{\text{non-driving}}$  is defined as the additional information processing cost resulted from the non-driving task. Hereafter, we define the  $TD(t)$  as the cumulative workload for the driver.

$$TD(t) = TD_{\text{car-following}}(t) + \sum_a TD_{\text{non-driving}}(t) \quad (3)$$

Hereafter,  $TS(t)$  is defined as the ratio of  $TD(t)$  and  $TC$  (we assume  $TC$  as the constant value of 1 in this paper). Meanwhile, it is reasonable for us to regard  $TS(t)$  as driver's task difficulty in this paper since  $TS(t)$  is the result of dynamic interactions between driver  $TD(t)$  and  $TC$ . When  $TS(t)$  is less than  $TC$ , the driver is capable of completing the current task safely and efficiently. While when  $TS(t)$  is close to  $TC$  or higher than  $TC$ , the driver may feel difficult to handle with his current task.

$$TS(t) = \frac{TD_{\text{car-following}}(t) + \sum_a TD_{\text{non-driving}}(t)}{TC} \quad (4)$$

Meanwhile, we also assume that the driver has the ability to withstand a certain overload, and driver can withstand up to two times the task demands of task capacity. In other words, if there exists secondary task (occupying a certain amount of information processing cost), the value of  $TS(t)$  may exceed  $TC$ , which may lead to the rapid deterioration of driver's SA.

Since the main concentration of this paper is to formulate the task difficulty of car-following task, the value of  $TD_{\text{car-following}}$  actually is equal to the value of  $TS(t)$  if there is no secondary task demands for the driver. For the convenience of subsequent research, we denote  $TD_{\text{car-following}}$  as  $TD_{cf}$ . In the next subsection, we will present the formulation of driver's driving task in the longitudinal direction.

### 2.3. Car-following task difficulty modeling

The theory of fuzzy logic algorithms originates from and is developed based on fuzzy mathematics, which overturns the limited concept of traditional mathematics that variables can only express 'one or the other'. By fuzzifying the input and output variables, the absolute membership in the classic set is blurred. In other words, the membership of element  $x$  in the set  $A$  is not limited to 0 or 1, but according to the membership function takes any value from 0 to 1.

$$\mu_A : U \rightarrow [0, 1] \quad (5)$$

$$x \rightarrow \mu_A(x) \quad (6)$$

Where  $A$  represents the fuzzy set defined on the universal set  $U$  and  $\mu_A(\cdot)$  is a membership function taking values 0-1. Thus, the fuzzy logic algorithm is capable of emulating human driver's behaviors through defining linguistic labels and setting fuzzy inference rules. Rather than using crisp values, using fuzzy rules is a quite suitable tool to model the driver's perception of his own task difficulty and the driver's situational awareness.

In order to model driver's driving task in the longitudinal direction using the fuzzy logic algorithm, we define three input variables,  $\{RP(t), RV(t), CV(t)\}$ , representing the relative position between leader and follower, the relative velocities between leader and follower and the current follower's velocity. Meanwhile, the output variable is defined as  $TD_{cf}(t)$  and the compact expression can be written as follows:

$$TD_{cf}(t) = F(RP(t), RV(t), CV(t)) \quad (7)$$

Where the instantaneous  $TD_{cf}(t)$  of driver at time  $t$  depends on the three input variables  $\{RP(t), RV(t), CV(t)\}$ . The mapping relationship  $F(\cdot)$  is determined by the fuzzy logic algorithm.

The input variables are divided into three fuzzy sets respectively, and the corresponding linguistic labels are given below. The assigned labels to the input variables are:  $RP(t)$ : small spacing, medium spacing, and large spacing; to the input  $RV(t)$ : leader's velocity is larger than follower's, leader's velocity is close to follower's, and leader's velocity is lower than follower's; to the input  $CV(t)$ : low velocity of follower, normal velocity of follower, and high velocity of follower.

$$RP(t) = \{\text{small}(SM), \text{medium}(ME), \text{large}(LG)\} \quad (8)$$

$$RV(t) = \{\text{negative}(NE), \text{zero}(ZE), \text{positive}(PO)\} \quad (9)$$

$$CV(t) = \{\text{low}(SL), \text{normal}(NR), \text{high}(HG)\} \quad (10)$$

The output variable is also divided into three fuzzy sets. The fuzzy set  $HG$  represents high level of task difficulty. The fuzzy set  $CT$  represents the critical level of task difficulty, below which the driver can easily handle the current driving task, and beyond which the driving task gradually become difficult for the driver.

$$TD_{cf}(t) = \{\text{average}(AV), \text{critical}(CT), \text{high}(HG)\} \quad (11)$$

Gaussian membership functions are selected for each fuzzy set, and the formula is given below. The reason why we choose this membership function is because this function contains two parameters: mean value  $\mu$  of  $TD_{cf}(t)$  and the variance  $\sigma$  of  $TD_{cf}(t)$ .

$$f(x) = e^{-\frac{(x-\mu)^2}{\sigma^2}} \quad (12)$$

Under the condition that  $\mu$  is fixed, different value of  $\sigma$  can be utilized to adjust the intersection area between two adjacent membership functions. As shown in Figure 3, in this area, the same value of  $RV(t)$  corresponds to two different Gaussian membership values (Value 1, Value 2), which is the main feature of fuzzy logic, reflecting the driver's ambiguous perception of the surrounding environment.



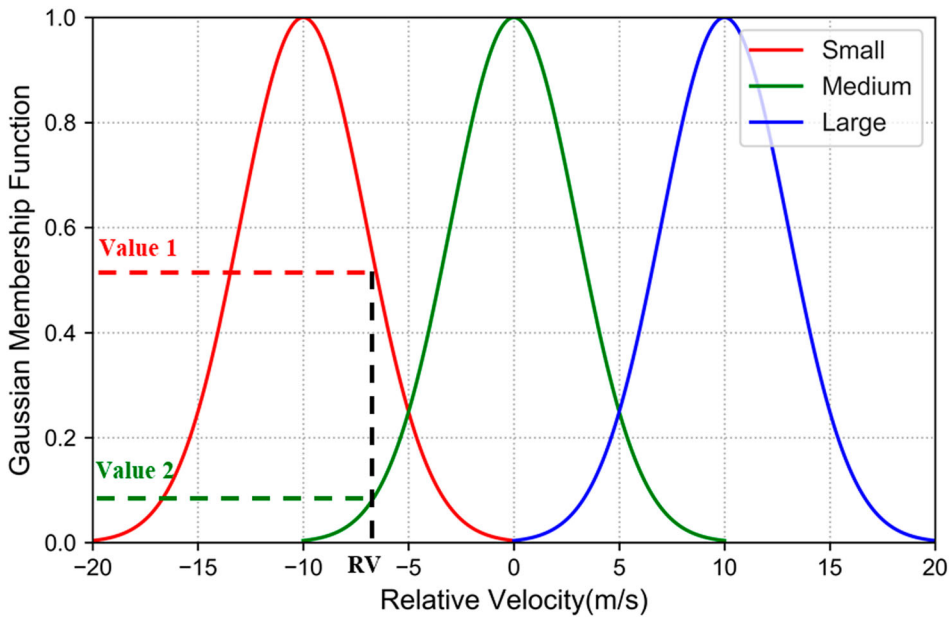


**Figure 3.** The Gaussian membership function of relative velocity with the leader vehicle.

**Table 1.** The fuzzy inference rules table of driving task difficulty.

Fuzzy set		Rules ( $3^3 = 27$ )							
RP	SM	SM	SM	SM	SM	SM	SM	SM	SM
RV	NE	NE	NE	ZE	ZE	ZE	PO	PO	PO
CV	SL	NR	HG	SL	NR	HG	SL	NR	HG
$TD_{cf}$	CT	CT	HG	CT	CT	HG	CT	HG	HG
RP	ME	ME	ME	ME	ME	ME	ME	ME	ME
RV	NE	NE	NE	ZE	ZE	ZE	PO	PO	PO
CV	SL	NR	HG	SL	NR	HG	SL	NR	HG
$TD_{cf}$	AV	CT	CT	AV	CT	CT	CT	CT	HG
RP	LG	LG	LG	LG	LG	LG	LG	LG	LG
RV	NE	NE	NE	ZE	ZE	ZE	PO	PO	PO
CV	SL	NR	HG	SL	NR	HG	SL	NR	HG
$TD_{cf}$	AV	AV	AV	AV	AV	CT	AV	CT	CT

After determining the fuzzy sets and membership function of the input and output variables, it is also important to enumerate the fuzzy inference rules. Since there are 3 inputs and 1 output, the number of fuzzy rules is  $3^3 = 27$  and the inference rule table is shown in Table 1.

## 2.4. Incorporation of task difficulty into LCM

In this subsection, we formulate the incorporation of driver's car-following task difficulty into the LCM, and then we derive the proposed FTD-LCM model. As mentioned above, the increase of driver's  $TS(t)$  may lead to the deterioration of driver's  $SA(t)$ . Therefore, it is also reasonable for us to employ the fuzzy logic approach to model the relationship between these two variables. The input variable  $TS(t)$  and output variable  $SA(t)$  are divided into 4 fuzzy sets, and their linguistic labels are given below.

$$TS(t) = \{\text{low } TS(A1), \text{average } TS(A2), \text{critical } TS(A3), \text{high } TS(A4)\} \quad (13)$$

$$SA(t) = \{\text{low } SA(B1), \text{critical } SA(B2), \text{average } SA(B3), \text{high } SA(B4)\} \quad (14)$$



The fuzzy set A1 represents the low level of  $TS(t)$ , the fuzzy set A2 represents the average level of  $TS(t)$ , the fuzzy set A3 represents the critical level of  $TS(t)$  whose value is close to 1, and the fuzzy set A4 represents the high level of  $TS(t)$  whose value exceeds 1. The fuzzy set B1 represents the low level of driver's perception of the surroundings (due to secondary tasks), the fuzzy set B2 represents the critical value of  $SA(t)$ , the fuzzy set B3 represents the average level of  $SA(t)$ , the fuzzy set B4 represents the high level of  $SA(t)$ . The Gaussian membership function is also introduced here. The fuzzy inference rules are determined here: A1 corresponds to B4, A2 corresponds to B3, A3 corresponds to B2, A4 corresponds to B1. The main reason for setting this is that we hope that  $SA(t)$  will maintain at a high level when  $TS(t)$  remains below  $TC$ . When  $TS(t)$  is close to  $TC$  or higher than  $TC$ ,  $SA(t)$  will decrease to a low level.

After obtaining the instantaneous value of  $SA(t)$ , we present the incorporation method (Van Lint and Calvert 2018) of this human factor into the LCM model. We define driver's perception error of the surrounding environment at time  $t$  as  $\sigma_{SA}(t)$ .

$$\sigma_{SA}(t) = SA_{\text{optimal}} - SA(t) \quad (15)$$

Where  $SA_{\text{max}}$  represents the optimal situational awareness for the driver.  $SA(t)$  represents the actual situational awareness for the driver. Therefore,  $\sigma_{SA}(t)$  represents driver's reduced SA from the optimal state.

It is reasonable for us to assume the deterioration of  $SA(t)$  may cause driver's perception errors of the surroundings. This kind of perception error may be reflected in the following:

$$\dot{x}_j^{\text{amend}} = \dot{x}_j + \delta_{SA}\sigma_{SA}(t)\dot{x}_j \quad (16)$$

$$s_{ij}^{\text{amend}}(t) = s_{ij}(t) + \delta_{SA}\sigma_{SA}(t)s_{ij}(t) \quad (17)$$

$$\Delta\dot{x}_{ij}^{\text{amend}}(t) = \Delta\dot{x}_{ij}(t) + \delta_{SA}\sigma_{SA}(t)\Delta\dot{x}_{ij}(t) \quad (18)$$

Where  $\dot{x}_j^{\text{amend}}$ ,  $s_{ij}^{\text{amend}}(t)$ ,  $\Delta\dot{x}_{ij}^{\text{amend}}(t)$  denote the modified parameters in the LCM model.  $\delta_{SA} = \text{sign}(\gamma)$  governs the direction of driver's perception bias (under- or overestimating the surrounding environment), where variable  $\gamma$  is evenly distributed between  $-1$  and  $1$  (For a deeper analysis of this parameter, please refer to Van Lint and Calvert (2018)).

In addition, the deterioration of driver's  $SA(t)$  would also affect driver's reaction time  $\tau_i^p$  and desired speed  $v_i$ .

$$\tau_i^{\text{amend}}(t) = \tau_i + \sigma_{SA}^2 \tau_i^{\text{max}} \quad (19)$$

$$v_i^{\text{amend}}(t) = v_i + \delta_{SA}\sigma_{SA}(t)v_i \quad (20)$$

Where  $\tau_i^{\text{amend}}(t)$ ,  $v_i^{\text{amend}}(t)$  denote the modified reaction time and desired speed.  $\tau_i^{\text{max}}$  is the maximum attention time lag. Note that we assume the magnitude of increase in reaction time is determined by  $\sigma_{SA}^2$  and  $\tau_i^{\text{max}}$  (2s).

Thus, driving (car-following) task difficulty has been incorporated into the underlying LCM model through transforming this into the deterioration of driver's situational awareness (modifying the parameters in the LCM). Overall, the detailed formulation of our proposed FTD-LCM model has been presented in this section. In the next section, we will present the numerical simulation of our proposed model.

### 3. Numerical experiments

#### 3.1. Scenario parameter settings

Assuming two-lane traffic flow in one direction, the Follower\_1 vehicle and the Leader vehicle (green vehicle) are 100 m apart, and keep a speed of 20 m/s at the beginning time. Each vehicle is under the control of a given CF model (FTD-LCM). After 30 s, the third vehicle (blue vehicle) suddenly cut in the

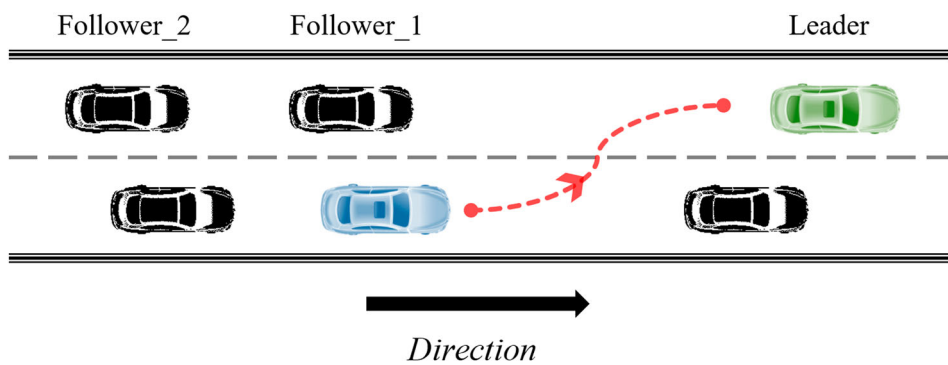


**Figure 4.** The schematic diagram of the numerical scenario.

**Table 2.** The mean value and variance of each fuzzy set in the numerical simulation.

Variable	Fuzzy set	Meaning of the fuzzy set	Membership function	Mean value	Variance
$RP(t)$	SM	Small spacing distance	Gaussian	20 m	10
	ME	Medium spacing distance	Gaussian	40 m	10
	LG	Larger spacing distance	Gaussian	80 m	10
$RV(t)$	NE	Negative difference	Gaussian	−15 m/s	5
	ZE	Zero difference	Gaussian	0 m/s	5
	PO	Positive difference	Gaussian	15 m/s	5
$CV(t)$	SL	Slow velocity	Gaussian	10 m/s	5
	NR	Normal velocity	Gaussian	20 m/s	5
	HG	High velocity	Gaussian	30 m/s	5
$TD_{cf}(t)$	AV	Average level of TD	Gaussian	0.4	0.05
	CT	Critical level of TD	Gaussian	0.8	0.05
	HG	High level of TD	Gaussian	1	0.05
$TS(t)$	A1	Low level of TS	Gaussian	0.3	0.2
	A2	Average level of TS	Gaussian	0.7	0.2
	A3	Critical level of TS	Gaussian	1	0.2
	A4	High level of TS	Gaussian	1.5	0.2
$SA(t)$	B1	Low level of SA	Gaussian	0.4	0.05
	B2	Critical level of SA	Gaussian	0.6	0.05
	B3	Average level of SA	Gaussian	0.9	0.05
	B4	High level of SA	Gaussian	1	0.05

lane ahead of the Follower\_1 vehicle with the speed of 20 m/s. The spacing between the Follower\_1 vehicle and the new leader vehicle is about 20 m at that time. It is worth noting that the LC (lane-changing) behavior has not been considered in the numerical simulation (it will be discussed in detail in the discussion). The numerical simulation ends in the 60 s, and the simulation timestep is 0.1 s. The schematic picture of the numerical simulation scenario is given in Figure 4.

The parameters of LCM are given respectively:  $\tau_i^p = 0.5$ ,  $b_i = 4 \text{ m/s}^2$ ,  $B_j = 3 \text{ m/s}^2$ ,  $A_i = 5 \text{ m/s}^2$ ,  $v_i = 30 \text{ m/s}$ ,  $L_i = 5 \text{ m}$ . The mean value and variance of each fuzzy set is given in Table 2. We assume the driver has the ability to withstand a certain overload, and driver can withstand up to two times the task demands of task capacity. Therefore, the range of  $TS(t)$  is set between 0-2. The average level of  $TS(t)$  is about 0.7, and the critical level of  $TS(t)$  is about 1, beyond which the driver's may feel difficult to hanle with his current taks demand. When  $TS(t)$  reaches about 1.5, this may cause a traffic accident. The average level of  $SA(t)$  is set about 0.9, and the critical level of  $SA(t)$  is set as 0.6, below which driver's situational awareness may deteriorate rapidly. On the other hand, cconsidering the basic driving competence (maintaining the car-following task) and the basic situational awareness for the driver, we assume the value of  $TD_{cf}(t)$  must not lower than 0.4, so as the value of  $SA(t)$ .

In order to evaluate the real-time risk in this numerical simulation, we introduce two safety indicators. One is the commonly-used TTC (Time to Collision) indicator, which is the ratio of the distance between two cars and their relative speed. Another indicator is called the 'Field Risk Indicator', which is originated from the Field Theory (Ni 2016b). This indicator represents the risk that the subject vehicle perceives on the road. It is more appropriate to quantify the risk than does TTC, since our underlying model is also derived from the Field Theory. For the convenience of subsequent analysis, we name this indicator as FRI (Field Risk Indicator). Therefore, in this paper, we both use these two indicators to quantify the real-time risk to provide more options, and the formulas are given below.

$$TTC(t) = \frac{s_{ij}(t) - L_j}{\dot{x}_i(t) - \dot{x}_j(t)} \quad (21)$$

$$FRI(t) = e^{\frac{s_{ij}^*(t) - s_{ij}(t)}{s_{ij}^*(t)}} \quad (22)$$

Where  $s_{ij}^* - s_{ij}$  represents the amount of the subject vehicle's intrusion into the leading vehicle's 'personal space'. Meanwhile it is worth noting that TTC only makes sense when  $\dot{x}_i(t)$  is larger than  $\dot{x}_j(t)$ , while the FRI indicator makes sense at any moment.

### 3.2. Simulation results

The numerical simulation results are shown in Figure 5. and it can be found that:

- (1) When the Follower\_1 gradually approaches the Leader, the value of driving task difficulty gradually increases from 0.6 to 0.8, and the corresponding value of situational awareness decreases from 0.9 to 0.8. This is mainly due to the gradual decrease of the spacing from 100 m to 35 m. The TTC value is higher than 10s and the FRI value remains below 0.5 over a period of the starting time.
- (2) When the Follower\_1 and the Leader maintained the safe spacing distance with the same speed, driver's driving task difficulty maintains at the level of 0.8 and driver's situational awareness maintains at the level of 0.9. Meanwhile, the reaction time gradually increased from 0.5 to 0.6. The additional 0.1s resulted from the decrease of driver's situational awareness.
- (3) When the blue vehicle suddenly cut in the lane ahead of the Follower\_1, the instantaneous driving task difficulty suddenly increased to 0.95 (approximately equal to driver's task capacity) due to the reduction of the spacing distance. Meanwhile, driver's situational awareness also changed suddenly, whose value decreased from 0.8 to 0.74. TTC decreased from 1.8s to 0.7s, FRI increased from 0.3 to 2.2, and the reaction time increased to 0.67s.

Incorporation of non-driving task demand is also considered here in order to present an illustration of the modeling procedure. We assume that the driver was answering the phone between 25s and 35s, which incurred a certain amount of information processing cost to the driver. Using the so-called fundamental diagram of task demand (Van Lint and Calvert 2018), we assume the constant information processing cost of answering the phone is about 0.3. The numerical simulation result is given in Figure 6. The yellow curve represents the additional information processing cost of the non-driving task (answering the phone), and the black curve represents the driver's total information processing costs (including the driving task and non-driving task). It can be found that:

- (1) At the moment driver answered his telephone, driver's task saturation reached at 1.07 (beyond driver's task capacity), and driver's situational awareness dropped from 0.88 to 0.67. At the same time, due to the impact of non-driving task, driver's reaction time increased from 0.5s to 0.72s.

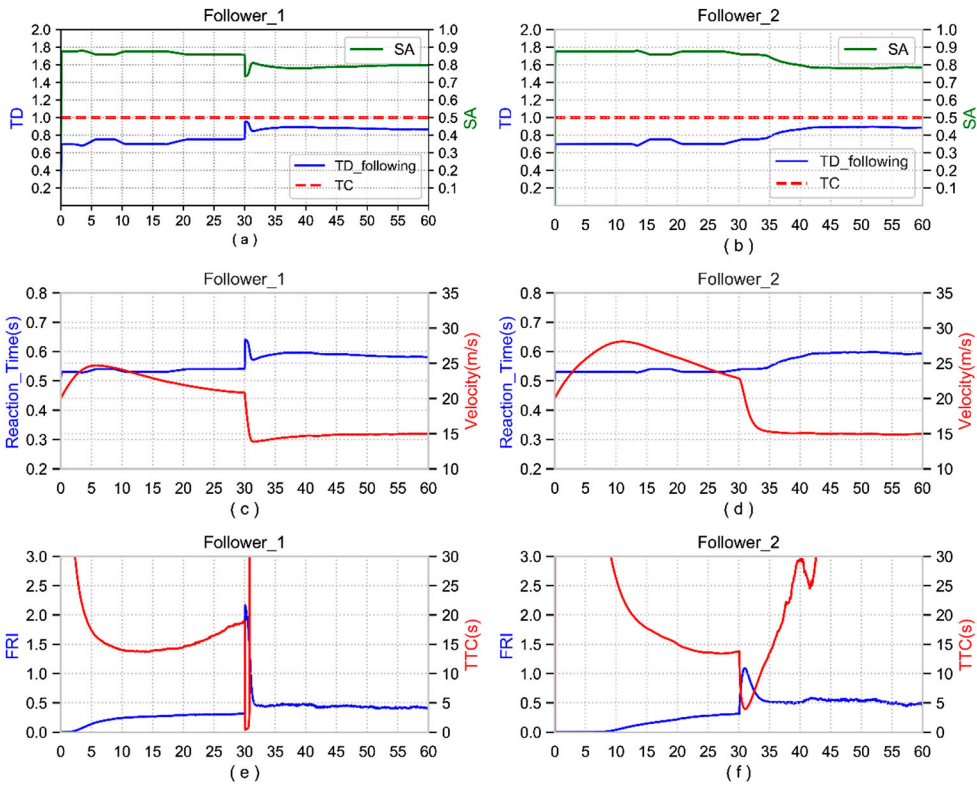


**Figure 5.** The tendency of parameters in numerical experiment considering no secondary task.

- (2) When the blue vehicle suddenly cut in the lane ahead of the Follower\_1, driver's task saturation instantly reached at 1.26. At that moment, the driver was actually overloaded due to the impact of both non-driving task and the instant increase of driving task difficulty. The driver's perception of the surrounding environment was greatly reduced at this time from 0.67 to 0.61. Correspondingly, driver's reaction time increased from 0.72s to 0.81s, the FRI increased from 0.31 to 2.2, and the value of TTC reached 0.6s.

Overall, we have presented detailed numerical simulation on our proposed FTD-LCM model in this section. The numerical results demonstrate that the both human factors of driving task demand and non-driving task demand have been successfully incorporated into our proposed model. In order to further evaluate the effectiveness, the next section will present the calibration of the proposed model using the field data.

## 4. Calibration preparation

### 4.1. Dataset and error correction

The data adopted in this paper comes from the famous Next Generation Simulation Program (NGSIM), which is supported by the Federal Highway Administration (FHWA). This well-known project is designed to develop a new generation of microscopic traffic simulation system. This database provides a series of high-fidelity individual microscopic trajectories. The original dataset contains all the trajectory information of all vehicles, including vehicle ID, lane number, time, speed, acceleration, vehicle class and space headway. Due to the inevitable systematic and discretization errors, it's necessary

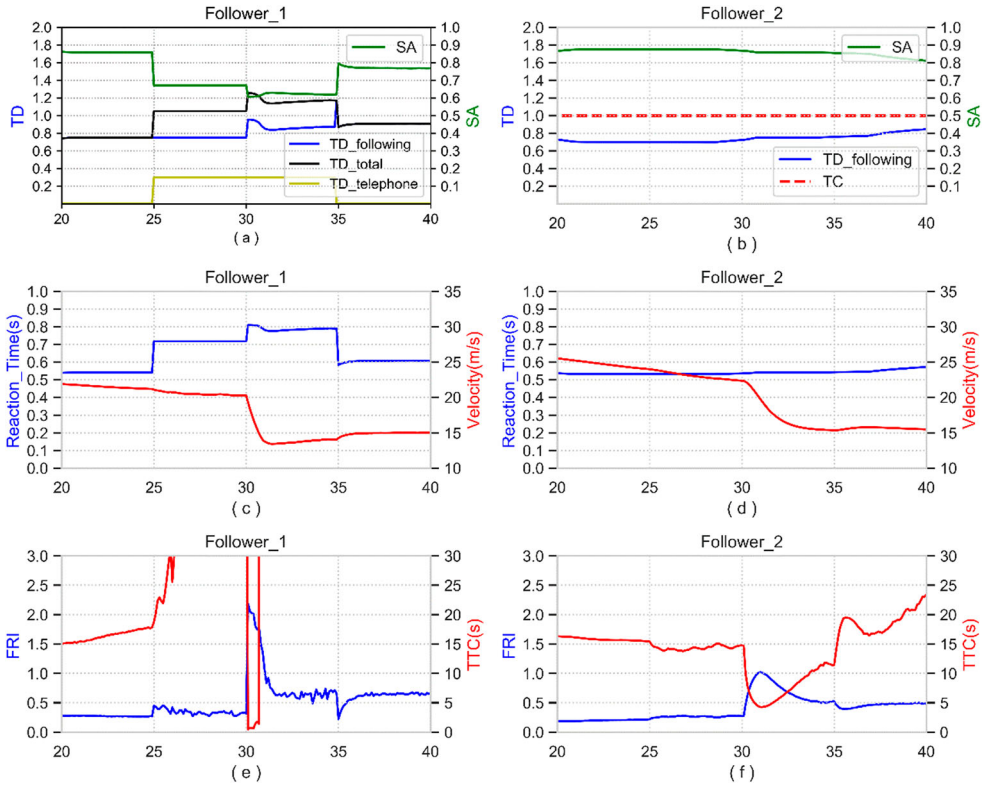


**Figure 6.** The tendency of parameters in numerical experiment considering secondary task.

for us to perform noise reduction on this dataset. Therefore, UKF (Unscented Kalman Filter) method is introduced to eliminate abnormal fluctuations. The reason why we choose this method is because that UKF is more suitable for denoising non-linear data with less computational cost (Julier and Uhlmann 2004; Chu, Saigal, and Saitou 2016). For the detailed formula of the UKF method, please refer to the Julier and Uhlmann (2004).

In this paper, we employ the data from the Interstate 80 in Emeryville (San Francisco), California. The selected time period is from 4:00 pm to 4:15 pm on 13 April 2005. We attempt to extract the CF trajectory data on the lane 2 in order to eliminate the influence of the on-ramp vehicle on the lane 7 (lane 2 is the innermost lanes). The time interval of this dataset is 0.1s.  $x(k) = [x(k), \dot{x}(k), \ddot{x}(k)]^T$  is defined as the state vector, where  $x(k)$  denotes the position,  $\dot{x}(k)$  denotes the acceleration, and  $\ddot{x}(k)$  denotes the velocity. The state transition matrix is defined as  $\begin{bmatrix} 1 & \Delta t & 0.5\Delta t^2 \\ 0 & 1 & \Delta t \\ 0 & 0 & 1 \end{bmatrix}$ , where  $\Delta t$  is the sampling interval.

Since the sampling time of the dataset is 0.1, we set  $\Delta t$  to 0.1. The measurement matrix is defined as  $\begin{bmatrix} 1 & 0 & 0 \end{bmatrix}$ , and the value of  $n_k$  is set as 0.04. The example of the denoising result is shown in Figure 7.

After denoising the original dataset, then we try to extract CF segments. The principles of extracting the segments are as follows: (1) The shortest time for CF trajectory must not be less than 30 s; (2) The data of the first and last 5 s of the CF trajectory are excluded to eliminate the effects of lane-changing. Finally, we extract 262 pairs of follower and leader trajectory. The examples of CF trajectories are shown in Figure 8, where blue curve represents the follower and red curve represents the leader. It is found that the trend of the follower's trajectory is highly similar to that of the leader both in position and velocity. Furthermore, the distribution of acceleration, velocity and space headway are shown in Figure 9.

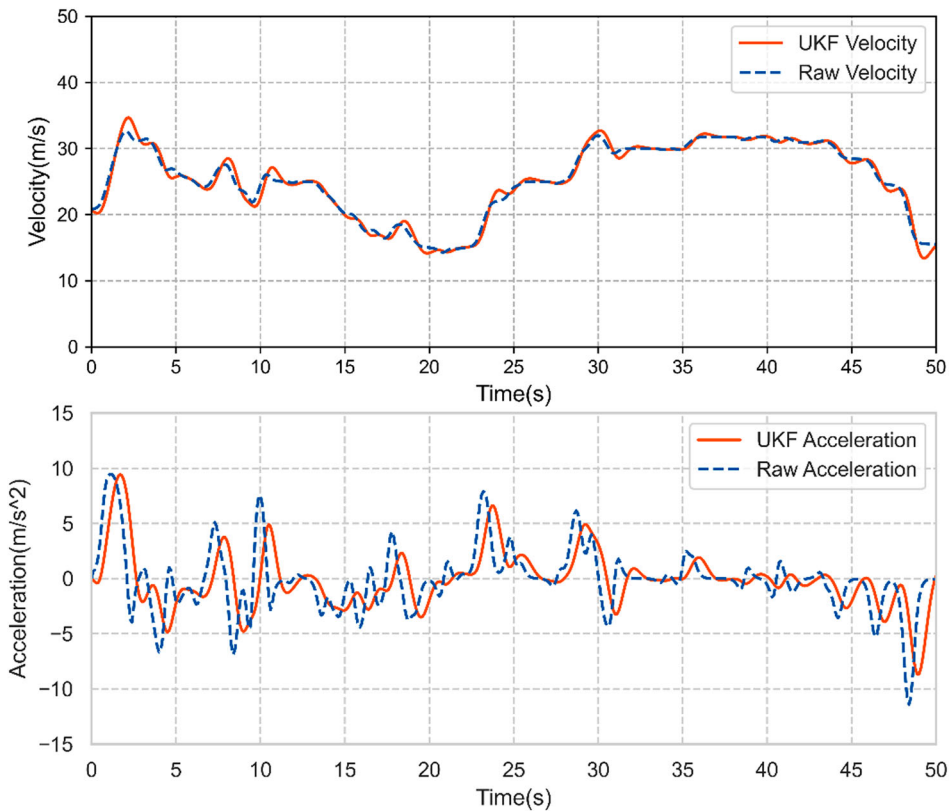


**Figure 7.** The denoising results between raw data and the processed data.

#### 4.2. Genetic algorithm preparation

Since the fuzzy logic algorithm is introduced to model driver's task difficulty and situational awareness, the proposed model contains many parameters to calibrate. On the other hand, the genetic algorithm is a powerful tool to find the optimum values of the model parameters, and has been often used in existing literature (Hao, Ma, and Xu 2016; Zhu, Wang, and Tarko 2018). Therefore, we will introduce the GA (Genetic Algorithm) to calibrate the proposed model.

The short description of the parameters needed to calibrate is shown in Table 3. The LCM model contains six parameters to calibrate. The parameters of the fuzzy sets RP, RV, CV and TD are used to reflect the degree of the task difficulty of the driving task. The parameters of the fuzzy set TS and SA are used to reflect the degree of the impact that the driver's instant task difficulty has on the driver's performance. Overall, there are total 32 parameters for us to calibrate.

The calibration can be considered as the learning process for the GA to search for the optimum parameters for the given object function. The main procedure of the GA consists of four steps: (1) Step 1: Randomly generate N chromosomes, crossover probability and mutation probability. Each individual represents a set of parameters corresponding to the objective function. (2) Step 2: Decode the corresponding parameters of each chromosome and determine the fitness of each chromosome through a predefined function. (3) Step 3: Perform crossover and mutation operations to generate new chromosomes for the next generation. The chromosomes that are more adaptive are more likely to crossover. (4) Step 4: Repeat the above steps 2 and 3 until the convergence requirements are met.

The calibration process of CF model is designed to minimize the difference between the actual CF trajectory and the simulated trajectory data generated by the CF model. In fact, any parameter



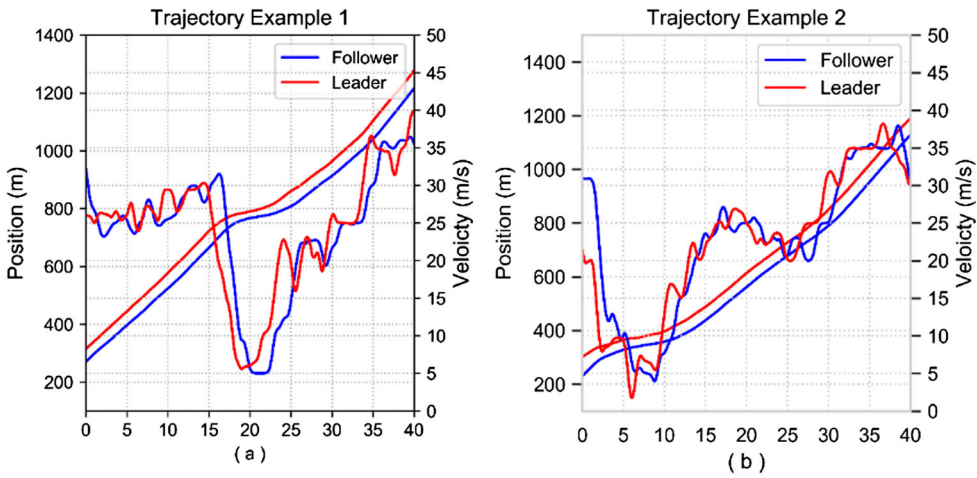


**Figure 8.** Examples of car-following trajectories which are extracted from the dataset.

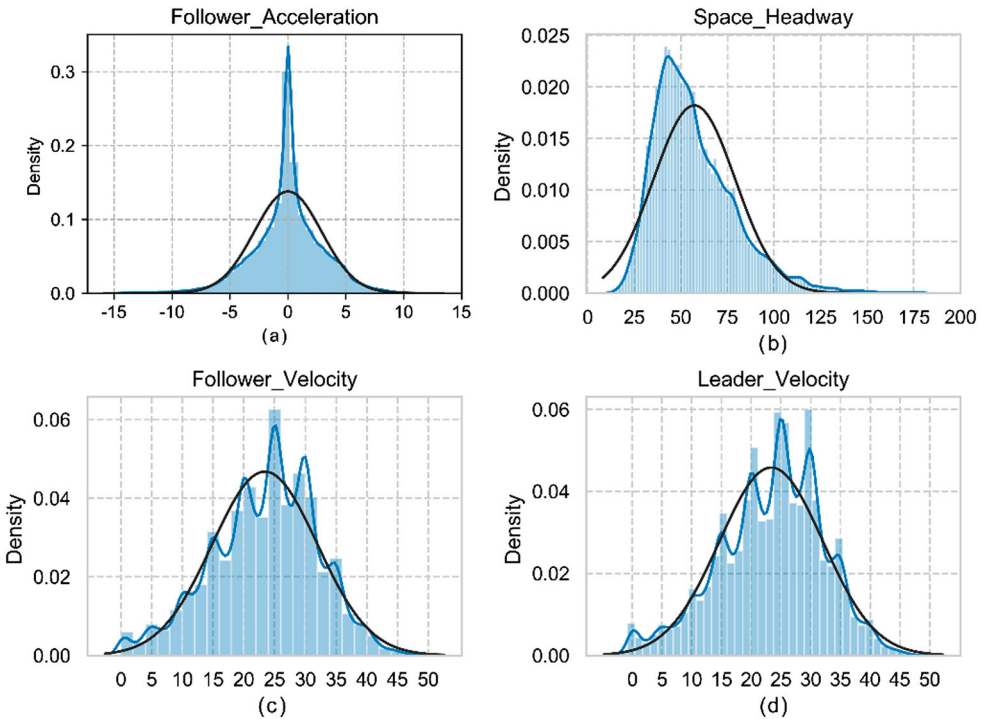


**Figure 9.** The acceleration, spacing and velocity distributions of the extracted CF trajectories dataset.

that represents driver's behavior can be utilized as the objective function or a part of the objective function, such as acceleration, velocity, space headway, time headway, etc. In this paper, we calibrate CF model at an individual level which means that the calibration process is repeated for each trajectory (Zhu, Wang, and Tarko 2018). For each trajectory, we input the actual velocities of the follower and the leader, and the actual spacing distance into the CF model. Hereafter, follower's acceleration could be obtained at each sampling interval. In this paper, we choose the following form of optimization



**Table 3.** A short description and the calibration range of the parameters in the FTD-LCM.

Parameters	Notation	Short description	Range [min, max]	Number
LCM	$b_i$	Driver's maximum deceleration	[4,10]	1
	$B_i$	Driver's estimation of leader's deceleration	[4,10]	1
	$A_i$	Driver's maximum acceleration	[4,10]	1
	$\tau_i$	Reaction time	[0.1,2]	1
	$v_i$	Desired speed	[15,30]	1
	$L_i$	Length of car	[4, 6]	1
Fuzzy set RP	$\mu_{RP}$	Mean value of SM, ME, LG	[0, 10], [35, 45], [70, 90]	4
	$\sigma_{RP}$	Variance of SM, ME, LG	[5, 10]	
Fuzzy set RV	$\mu_{RV}$	Mean value of NE, ZE, PO	[−20, −10], [−3, 3], [10, 20]	4
	$\sigma_{RV}$	Variance of NE, ZE, PO	[3, 7]	
Fuzzy set CV	$\mu_{CV}$	Mean value of SL, NR, HG	[5, 15], [15, 25], [25, 35]	4
	$\sigma_{CV}$	Variance of NE, ZE, PO	[3,7]	
Fuzzy set TD	$\mu_{TD}$	Mean value of AV, CT, HG	[0.4, 0.6], [0.7, 0.8], [0.9, 1]	4
	$\sigma_{TD}$	Variance of AV, CT, HG	[0.01, 0.1]	
Fuzzy set TS	$\mu_{TS}$	Mean value of A1, A2, A3, A4	[0, 0.3], [0.5, 0.9], [0.9, 1.5], [1.5, 2]	5
	$\sigma_{TS}$	Variance of A1, A2, A3, A4	[0.1, 0.3]	
Fuzzy set SA	$\mu_{SA}$	Mean value of B1, B2, B3, B4	[0.5, 0.6], [0.6, 0.7], [0.7, 0.9], [0.9, 1]	5
	$\sigma_{SA}$	Variance of B1, B2, B3, B4	[0.01, 0.08]	

objective function, which has a more balancing measure weighting (Kurtc and Treiber 2016).

$$\min J(a_i^{\text{simu}}, a_i^{\text{real}}) = \frac{\sum_{i=1}^n (a_i^{\text{simu}} - a_i^{\text{real}})^2 / |a_i^{\text{real}}|}{\sum_{i=1}^n |a_i^{\text{real}}|} \quad (23)$$

Where  $a_i^{\text{real}}$  represents the true data and  $a_i^{\text{simu}}$  represents the simulated data.

## 5. Calibration results and discussion

### 5.1. Calibration results

This section presents the calibration and validation of the proposed CF model. It is undeniable that this dataset has certain limitations. However, it is still advisable for us to verify the effectiveness of this model in reflecting the actual traffic characteristics (detailed discussion will be presented in the next section). Furthermore, the comparison with its predecessor model is also conducted here so as to evaluate the performance of our proposed model. We randomly select 257 trajectories as the calibration dataset and the remaining 5 trajectories are selected as the validation dataset. We use the GA embedded in the Scikit-Opt package in Python. We set the initial population to 200, the maximum iteration to 200, the intersection probability to 0.95 and the mutation probability to 0.05.

The boxplot distribution (objective function values) of FTD-LCM and LCM are given in Figure 10. It can be found that the objective function values are roughly distributed between 2 and 12. Although the median value of LCM is lower than the median value of FTD-LCM, our proposed model has fewer larger values and has more smaller values than that of LCM, which demonstrates that our proposed model performs better than its predecessor in the calibration results. On the other hand, since we calibrate the task difficulty of driving task, we could obtain the relationship between relative position, relative velocity, current velocity and driving task difficulty (in Figure 11). It can be found that with the decrease of RP or increase of RV or the increase of CV, driver's driving task would gradually increase, which indicates that the human factor of driving task difficulty is well reflected in our proposed model. The calibration summaries of the parameters in LCM and FTD-LCM are given in Tables 4 and 5.

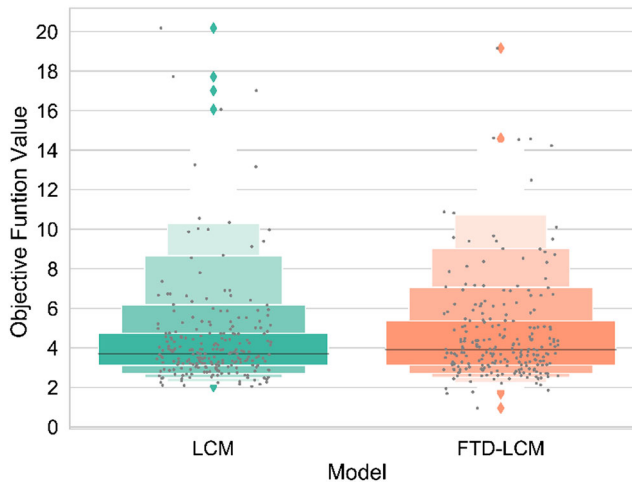


**Figure 10.** The boxplot distribution results of the objective function values of LCM and FTD-LCM.

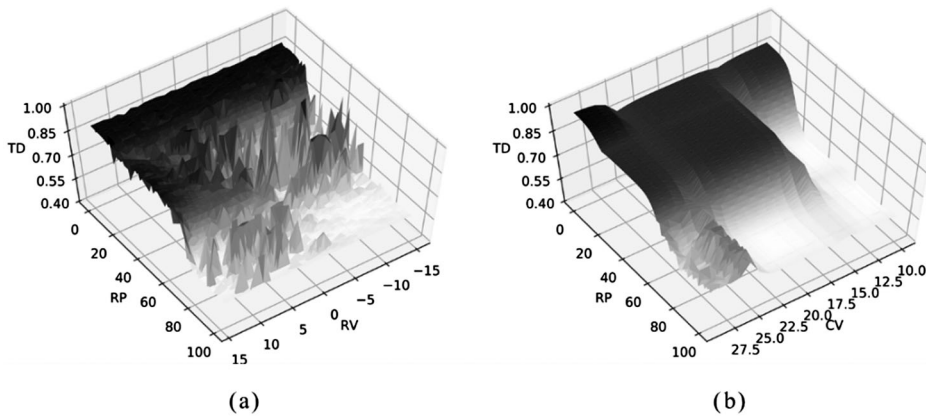


**Figure 11.** The fuzzy relation among RP, RV, CV with Driving Task.

## 5.2. Validation results

Hereafter, the remaining five trajectories are utilized to validate the LCM model and our proposed model. We choose the mean value of each parameter in Tables 4 and 5 as the corresponding parameter to validate the remaining trajectories. The error indicators: MAE (Mean Absolute Error), MSE (Mean Squared Error), RMSE (Root Mean Squared Error) are introduced to evaluate the performance of validation results. The validation comparison result (Figure 12) demonstrates that the MAE, MSE, RMSE values of our proposed model are all lower than those of the LCM (the acceleration generated by the LCM model and the FTD-LCM model). The corresponding trajectory curve is shown in Figure 13. The blue line represents the actual trajectory, the green line represents the trajectory generated by the LCM model, and the orange line represents the trajectory generated by our proposed model. The results demonstrate that both the trajectory generated by LCM and FTD-LCM are coincide with the actual trajectory data, while our proposed model exhibits better performance than its predecessor (unrealistic position of the follower vehicle). Although there are some deviations at certain situations, the simulated trajectory of our proposed model is consistent with the actual data everywhere else.

**Table 4.** Summary of the FTD-LCM parameters in calibration.

Notation	Median	Mean	Std. dev.	Notation	Median	Mean	Std. dev.
$b_i$	6.269	6.143	1.206	$\mu_{CV}^{HG}$	30.624	30.383	2.823
$B_i$	5.922	5.95	1.199	$\sigma_{CV}$	6.941	7.008	0.603
$A_i$	2.438	2.809	0.941	$\mu_{TD}^{AV}$	0.496	0.502	0.053
$\tau_i$	0.401	0.457	0.284	$\mu_{TD}^{CT}$	0.745	0.745	0.029
$v_i$	25.751	24.654	4.558	$\mu_{TD}^{HG}$	0.945	0.946	0.024
$L_i$	5.045	5.031	0.592	$\sigma_{TD}$	0.046	0.042	0.023
$\mu_{RP}^{SM}$	5.452	5.428	2.85	$\mu_{TS}^{A1}$	0.139	0.142	0.086
$\mu_{RP}^{ME}$	40.313	40.696	3.071	$\mu_{TS}^{A2}$	0.697	0.696	0.105
$\mu_{RP}^{LG}$	79.615	78.928	6.099	$\mu_{TS}^{A3}$	1.253	1.259	0.142
$\sigma_{RP}$	7.521	7.449	1.552	$\mu_{TS}^{A4}$	1.741	1.735	0.131
$\mu_{RV}^{NE}$	−15.092	−15.291	3.136	$\sigma_{TS}$	0.236	0.228	0.029
$\mu_{RV}^{ZE}$	−0.143	−0.336	1.927	$\mu_{SA}^{B1}$	0.517	0.513	0.012
$\mu_{RV}^{PO}$	15.306	14.879	2.818	$\mu_{SA}^{B2}$	0.608	0.601	0.039
$\sigma_{RV}$	4.826	4.697	1.307	$\mu_{SA}^{B3}$	0.839	0.848	0.049
$\mu_{CV}^{SL}$	8.927	8.513	2.678	$\mu_{SA}^{B4}$	0.956	0.956	0.028
$\mu_{CV}^{NR}$	21.017	21.518	2.506	$\sigma_{SA}$	0.075	0.076	0.002

**Table 5.** Summary of the LCM parameters in calibration.

Parameter	Bounds	25%	75%	Mean	Medium	Std. dev.
$v_i$	[15,30]	28.597	29.910	28.367	29.530	2.886
$A_i$	[4, 10]	4.011	4.190	4.194	4.047	0.488
$\tau_i$	[0.1, 2]	0.865	1.523	1.178	1.158	0.442
$L_i$	[4, 6]	4.629	5.277	4.949	4.898	0.338
$b_i$	[4, 10]	7.081	9.636	8.196	8.771	1.717
$B_i$	[4, 10]	8.175	9.481	8.705	9.028	1.038

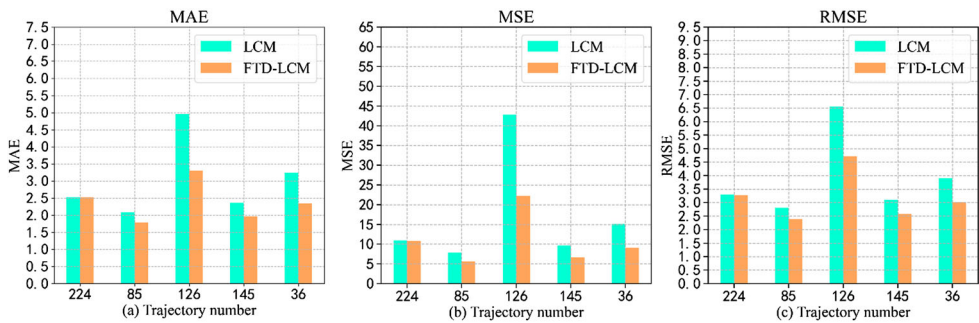


**Figure 12.** Validation results of the LCM and the FTD-LCM.

## 6. Discussion

The center of this research is to incorporate human factors into the existing CF models. The establishment of our proposed model is in the context of our attempts to address the three existing research gaps as elaborated in the Introduction. We have made the first attempt to combine the TCI model, LCM model and the fuzzy logic approach together in this paper. One may argue that the efforts of such combination seem to be trivial. However, what' really matters and worth our attention is the deep

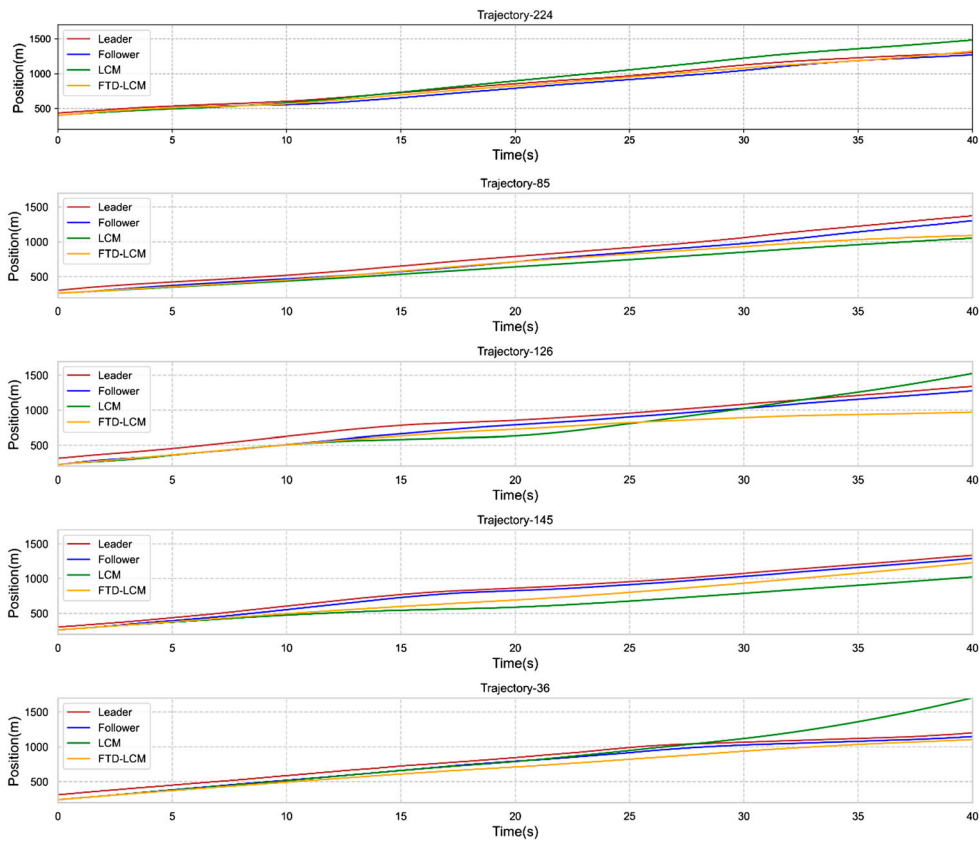


**Figure 13.** The comparison between the actual and simulated trajectories.

consideration behind this combination (why we choose these approaches, what are their current limitations, and why they could blend together), which should deserve our comprehensive thinking and exploring. And this is exactly the real motivation and contribution of this paper. Through fusing these approaches together, our proposed model has greater potential for reflecting the essential characteristics of traffic flow phenomena, since the fused model breaks through the deficiencies of the original model, while inheriting the merits of the original model, thus shedding light on the future development of CF models. Thereafter, the effectiveness of our proposed model has been verified both in the numerical simulation and field-data validation.

The field-data calibration and validation results suggest that our proposed model could achieve better performance than its predecessor in reproducing actual traffic flow phenomena. This indicates that our proposed model has greater capability of capturing the mechanism of traffic flow characteristic from the trajectory data. This may be largely due to the model fusion done in this research (overcoming the disadvantages and absorbing the merits of each approach). In other words, the LCM model, the TCI model and the fuzzy approach could fit together very well (more human factors have been incorporated into the LCM model, a desirable underlying model has been employed for the TCI model, and a more reasonable approach of modeling the task difficulty has been adopted). In short, we have successfully incorporated the Risk Allostasis Theory (Fuller 2005, 2011) into the LCM model, and the main concentration of this paper is modeling the driving task difficulty in the longitudinal direction. Meanwhile, the illustration of modeling the non-driving task has also been confirmed in the numerical simulation using the FDTD (fundamental diagram of task demand) (Van Lint and Calvert 2018; Calvert, Schakel, and van Lint 2020). One may argue that the computational cost is relatively high since there

are more parameters needed to calibrate after the fusion of these approaches, thus making it difficult for us to adopt this model in the real traffic flow environment. However, the calibration and the validation results suggest that the sacrifice of the increase of the degree of parameter freedoms seems worthwhile, since the proposed model is more capable of accommodating more human factors, and it is indeed necessary for us to take more human factors into account. And whenever we attempt to incorporate more human factors into the existing CF models, it is inevitable that the complexity of the underlying model parameters would increase (more parameters are needed to capture various human factors). In fact, this relates to the trade-off between our desire for more incorporation of human factors and our desire for a simpler model to be used in the reality. How to balance such trade-off should be further considered in the follow-up development of this research.

In general, incorporation of human factors into the existing mathematical CF models (as the core of CF driving behavior) is crucial for us not only to model various complex driving behaviors more accurately, but also assist us to acquire a full understanding of traffic flow phenomenon. Therefore, we have established a novel CF model which attempts to incorporate the role of task difficulty in human driving in this paper. However, many aspects of this paper need further research. First, we simply assume the new leader vehicle suddenly cut in the lane ahead of the following vehicle without considering the influence of the LC (lane-changing) behavior in the numerical simulation. However, along with CF behavior, LC behavior is also an indispensable part of traffic flow theory (Zhang, Sun, and Qi 2019) for us to get a more comprehensive understanding of the characteristics of traffic flow (Van Lint and Calvert 2018). Therefore, researching on how to model the task difficulty of LC is also as important as that of CF. Since LC action of the subject vehicle involves the longitudinal and lateral movement, future research may employ the distance between these two directions or more variables for modeling the task difficulty of LC. To be more specific, this may involve the research of LC trajectory planning algorithm and LC trajectory tracking algorithm (Luo et al. 2016; Yang, Zheng, and Wen 2018). Therefore, future research may try to integrate CF task difficulty and LC task difficulty together in order to achieve the formulation of task difficulty both in the longitudinal and lateral direction simultaneously. Second, the NGSIM dataset used in this article has certain limitations. One is the inevitable systematic and discretization errors in the dataset (Coifman and Li 2017). The other is that this dataset may not well reflect the characteristics of driver's task difficulty. Though it is unknown whether the trajectory data has already reflected driver's task difficulty, it is at least not appropriate to preclude the possibility. However, it is undeniable that the dataset used in this paper indeed has certain limitations. Therefore, how to collect the dataset that could better reflect the feature about driver's task difficulty may become one of the key directions of the future research of this study. Third, driver's driving task (car-following) difficulty may be affected by the multiple vehicles ahead (not just the vehicle ahead). Actually, there are already many researches which take this into account (Peng and Sun 2010; Guo et al. 2017; Wu, Wang, and Li 2020). Therefore, how to model the influence of multiple vehicles ahead on driver's task difficulty may become one of the future works of this research, and it will inevitably involve the second point we mentioned above (the collection and calibration of the dataset).

## 7. Conclusion

In this paper, a novel CF model is developed to imitate the human driver. The establishment of our model is in the context of our attempts to improve these three limitations: the demand for more inclusion of human factors into the LCM, the requirement for a more desirable underlying CF model for the framework of the TCI model, and the ignorance of the fuzziness of human brains when modeling driver's task difficulty. It is these underlying motivations behind the combination of these approaches that prompt us to develop this model in order to model the CF behavior more accurately. Specifically, under the framework of TCI model, the fuzzy logic approach is employed to formulate driver's natural or subjective driving task difficulty (using the relative position, relative velocity, and current velocity) in the longitudinal direction. Hereafter, (car-following) task difficulty is incorporated into the underlying LCM model through transforming the task difficulty into the deterioration of driver's situational

awareness. In order to evaluate our proposed model, we have conducted both numerical experiment (including considering driving/ non-driving task demand) and field-data calibration. Results demonstrate the effectiveness of our proposed model in replicating driver's CF task difficulty. Meanwhile, results also indicate that our proposed model exhibits better performance than its predecessor in reflecting actual traffic phenomena. Overall, we hope this model maybe useful for the enhancement of incorporation of human factors into existing CF models.

## Acknowledgements

Authors thank the anonymous reviewers for their constructive comments and help to improve our paper.

## Disclosure statement

No potential conflict of interest was reported by the author(s).

## Funding

This work was supported by National Key Research and Development Program of China [grant number 2018YFE0102800].

## References

- Andersen, G. J., and C. W. Sauer. 2007. "Optical Information for Car Following: The Driving by Visual Angle (dva) Model." *Human Factors* 49 (5): 878–896.
- Bando, M., K. Hasebe, A. Nakayama, et al. 1995. "Dynamical Model of Traffic Congestion and Numerical Simulation." *Physical Review E* 51 (2): 1035.
- Batool, W., M. M. Mubasher, and S. W. ul Qounian. 2019. "Modeling Task Capability in Full Velocity Differential Model." 2019 2nd International Conference on Advancements in Computational Sciences (ICACS).
- Brackstone, M., and M. McDonald. 1999. "Car-following: A Historical Review." *Transportation Research Part F: Traffic Psychology and Behaviour* 2 (4): 181–196.
- Calvert, S. C., W. J. Schakel, and J. W. C. van Lint. 2020. "A Generic Multi-Scale Framework for Microscopic Traffic Simulation Part II – Anticipation Reliance as Compensation Mechanism for Potential Task Overload." *Transportation Research Part B: Methodological* 140: 42–63.
- Calvert, S. C., and B. Van Arem. 2020. "A Generic Multi-Level Framework for Microscopic Traffic Simulation with Automated Vehicles in Mixed Traffic." *Transportation Research Part C: Emerging Technologies* 110: 291–311.
- Chen, J., R. Liu, D. Ngoduy, et al. 2016. "A New Multi-Anticipative Car-Following Model with Consideration of the Desired Following Distance." *Nonlinear Dynamics* 85 (4): 2705–2717.
- Chu, K. C., R. Saigal, and K. Saitou. 2016. "Stochastic Lagrangian Traffic Flow Modeling and Real-Time Traffic Prediction." 2016 IEEE International Conference on Automation Science and Engineering (CASE), 21–25 Aug. 2016.
- Coifman, B., and L. Li. 2017. "A Critical Evaluation of the Next Generation Simulation (Ngsim) Vehicle Trajectory Dataset." *Transportation Research Part B: Methodological* 105: 362–377.
- Endsley, M. R. 1995. "Toward a Theory of Situation Awareness in Dynamic Systems." *Human Factors* 37 (1): 32–64.
- Fritzsche, H. T. 1994. "A Model for Traffic Simulation." *Traffic Engineering and Control* 35 (5): 317–321.
- Fuller, R. 2005. "Towards a General Theory of Driver Behaviour." *Accident Analysis & Prevention* 37 (3): 461–472.
- Fuller, R. 2011. "Driver Control Theory: From Task Difficulty Homeostasis to Risk Allostasis." In *Handbook of Traffic Psychology*, edited by Bryan E. Porter, 13–26. San Diego, California, USA: Elsevier.
- Gazis, D. C., R. Herman, and R. W. Rothery. 1961. "Nonlinear Follow-the-Leader Models of Traffic Flow." *Operations Research* 9 (4): 545–567.
- Gipps, P. G. 1981. "A Behavioural Car-Following Model for Computer Simulation." *Transportation Research Part B: Methodological* 15 (2): 105–111.
- Guo, L., X. Zhao, S. Yu, et al. 2017. "An Improved Car-Following Model with Multiple Preceding Cars' Velocity Fluctuation Feedback." *Physica A: Statistical Mechanics and its Applications* 471: 436–444.
- Hao, H., W. Ma, and H. Xu. 2016. "A Fuzzy Logic-Based Multi-Agent Car-Following Model." *Transportation Research Part C: Emerging Technologies* 69: 477–496.
- Hoogendoorn, R., B. Van Arem, S. Hoogendoorn, et al. 2013. "Applying the Task-Capability-Interface Model to the Intelligent Driver Model in Relation to Complexity." In *Transportation Research Board 92nd Annual Meeting*. Washington DC, United States.
- Jiang, R., Q. Wu, and Z. Zhu. 2001. "Full Velocity Difference Model for a Car-Following Theory." *Physical Review E* 64 (1): 017101.
- Julier, S. J., and J. K. Uhlmann. 2004. "Unscented Filtering and Nonlinear Estimation." *Proceedings of The IEEE* 92 (3): 401–422.



- Khodayari, A., R. Kazemi, A. Ghaffari, et al. **2011**. "Design of an Improved Fuzzy Logic Based Model for Prediction of Car Following Behavior." *2011 IEEE International Conference on Mechatronics*.
- Kurtz, V., and M. Treiber. **2016**. "Calibrating the Local and Platoon Dynamics of Car-Following Models on the Reconstructed Ngsim Data." In *Traffic and Granular flow'15*, edited by Victor L. Knoop and Winnie Daamen, 515–522. Cham: Springer.
- Luo, Y., Y. Xiang, K. Cao, et al. **2016**. "A Dynamic Automated Lane Change Maneuver Based on Vehicle-to-Vehicle Communication." *Transportation Research Part C: Emerging Technologies* 62: 87–102.
- Ni, D. **2016a**. "Chapter 12 – Microscopic Modeling." In *Traffic Flow Theory*, edited by Daiheng Ni, 177–184. Amherst, Massachusetts, USA: Butterworth-Heinemann.
- Ni, D. **2016b**. "Chapter 21 – The Field Theory." In *Traffic Flow Theory*, edited by Daiheng Ni, 287–310. Amherst, Massachusetts, USA: Butterworth-Heinemann.
- Ni, D., J. D. Leonard, C. Jia, et al. **2015**. "Vehicle Longitudinal Control and Traffic Stream Modeling." *Transportation Science* 50 (3): 1016–1031.
- Ossen, S., and S. P. Hoogendoorn. **2006**. "Multi-Anticipation and Heterogeneity in Car-Following Empirics and a First Exploration of Their Implications." *2006 IEEE Intelligent Transportation Systems Conference*.
- Peng, G. H., and D. H. Sun. **2010**. "A Dynamical Model of Car-Following with the Consideration of the Multiple Information of Preceding Cars." *Physics Letters A* 374 (15–16): 1694–1698.
- Pipes, L. A. **1953**. "An Operational Analysis of Traffic Dynamics." *Journal of Applied Physics* 24 (3): 274–281.
- Precht, L., A. Keinath, and J. F. Krems. **2017**. "Identifying Effects of Driving and Secondary Task Demands, Passenger Presence, and Driver Characteristics on Driving Errors and Traffic Violations—Using Naturalistic Driving Data Segments Preceding Both Safety Critical Events and Matched Baselines." *Transportation Research Part F: Traffic Psychology And Behaviour* 51: 103–144.
- Przybyla, J., J. Taylor, J. Jupe, et al. **2012**. "Simplified, Data-Driven, Errorable Car-Following Model to Predict the Safety Effects of Distracted Driving." *2012 15th International IEEE Conference on Intelligent Transportation Systems*.
- Reuschel, A. **1950**. "Fahrzeugbewegungen in der Kolonne." *Osterreichisches Ingenieur Archiv* 4: 193–215.
- Saifuzzaman, M., and Z. Zheng. **2014**. "Incorporating Human-Factors in car-Following Models: A Review of Recent Developments and Research Needs." *Transportation Research Part C: Emerging Technologies* 48: 379–403.
- Saifuzzaman, M., Z. Zheng, M. M. Haque, et al. **2015**. "Revisiting the Task–Capability Interface Model for Incorporating Human Factors Into car-Following Models." *Transportation Research Part B: Methodological* 82: 1–19.
- Saifuzzaman, M., Z. Zheng, M. M. Haque, et al. **2017**. "Understanding the Mechanism of Traffic Hysteresis and Traffic Oscillations Through the Change in Task Difficulty Level." *Transportation Research Part B: Methodological* 105: 523–538.
- Treiber, M., A. Kesting, and D. Helbing. **2006**. "Delays, Inaccuracies and Anticipation in Microscopic Traffic Models." *Physica A: Statistical Mechanics and its Applications* 360 (1): 71–88.
- Van Lint, J., and S. Calvert. **2018**. "A Generic Multi-Level Framework for Microscopic Traffic Simulation – Theory and an Example Case in Modelling Driver Distraction." *Transportation Research Part B: Methodological* 117: 63–86.
- Van Lint, H., S. Calvert, W. Schakel, et al. **2017**. "Exploring the Effects of Perception Errors and Anticipation Strategies on Traffic Accidents – A Simulation Study." *International Conference on Applied Human Factors and Ergonomics*.
- Wickens, C. D., J. G. Hollands, and S. Banbury. **2015**. *Engineering Psychology and Human Performance*. New York: Psychology Press.
- Wiedemann, R. **1974**. "Simulation des Strassenverkehrsflusses." *Traffic Engineering*. University of Karlsruhe.
- Wu, B., W. Wang, L. Li, et al. **2020**. "Longitudinal Control Model for Connected Autonomous Vehicles Influenced by Multiple Preceding Vehicles." *Journal of Traffic and Transportation Engineering* 20 (02): 184–194.
- Yang, H. H., and H. Peng. **2010**. "Development of an Errorable Car-Following Driver Model." *Vehicle System Dynamics* 48 (6): 751–773.
- Yang, D., S. Zheng, C. Wen, et al. **2018**. "A Dynamic Lane-Changing Trajectory Planning Model for Automated Vehicles." *Transportation Research Part C: Emerging Technologies* 95: 228–247.
- Zhang, X., J. Sun, X. Qi, et al. **2019**. "Simultaneous Modeling of Car-Following and Lane-Changing Behaviors Using Deep Learning." *Transportation Research Part C: Emerging Technologies* 104: 287–304.
- Zhu, M., X. Wang, and A. Tarko. **2018**. "Modeling Car-Following Behavior on Urban Expressways in Shanghai: A Naturalistic Driving Study." *Transportation Research Part C: Emerging Technologies* 93: 425–445.